*Inorg. Chem.* **2008**, *47*, 7133−7138

# Two Dawson-Templated Three-Dimensional Metal−Organic Frameworks Based on Oxalate-Bridged Binuclear Cobalt(II)/Nickel(II) SBUs and Bpy Linkers

**Xinyu Zhao, Dadong Liang, Shuxia Liu,* Chunyan Sun, Ruige Cao, Chaoying Gao, Yuanhang Ren, and Zhongmin Su***

*Key Laboratory of Polyoxometalates Science of Ministry of Education, College of Chemistry, Northeast Normal University, Changchun City, JiLin, PRC 130024*

Received January 23, 2008

The Dawson anion $P_2W_{18}O_{62}^{6-}$ has been used as a noncoordinating polyoxoanion template for the construction of two metal−organic frameworks, namely, $[M_2(bpy)_3(H_2O)_2(ox)][P_2W_{18}O_{62}]2(H_2\text{-bpy}) \cdot nH_2O$ (M = Co(II), $n = 3$ (**1**); M = Ni(II), $n = 2$ (**2**)) (bpy = 4,4′-bipyridine; ox = $C_2O_4^{2-}$). Single-crystal X-ray analysis reveals that both of the structures exhibit 3D host frameworks constructed from the oxalate-bridged binuclear superoctahedron secondary building units (SBUs) and bpy linkers and the voids of which are occupied by Dawson anions, guest bpy, and water molecules. Magnetic studies reveal that there are antiferromagnetic exchange interactions among the transition-metal centers in compounds **1** and **2**. Furthermore, a compound **1**-modified carbon paste electrode (**1**-CPE) displays good electrocatalytic activity toward the reduction of nitrite.

## Introduction

Because of their controllable and adjustable pore sizes/shapes and chemical functionalities, metal−organic frameworks (MOFs) are regarded as promising materials for applications in catalysis, separation, gas storage, and molecular recognition.[1] Designing and constructing these kinds of materials by a template approach has become an important trend in synthetic chemistry.[2] In this field, various anions have been introduced as templates to direct the formation of porous frameworks containing various transition-metal ions bridged by multitopic ligands.[3] The incorporation of polyoxometalates (POMs) as anion templates is particularly attractive for two reasons: (a) they possess a remarkable chemical and structural diversity, which offers us the opportunity to control and adjust the pore sizes/shapes of MOFs, and (b) there is a large amount of research activity concerning their practical applications, especially in heterogeneous and homogeneous catalysis and in medicine.[4] So far, much work is focused on the construction of POMs-based coordination polymers through the direct incorporation of POMs into the network by covalent bonds.[2b,5–7] However, the examples of the construction of MOFs with the noncoordinating POMs template are based on several kinds of

* To whom correspondence should be addressed. E-mail: liusx@nenu.edu.cn (S.L.), zmsu@nenu.edu.cn (Z.S.). Fax: +86-431-85099328.

(1) (a) Thomas, J. M. *Philos. Trans. R. Soc. London, Ser. A* **1990**, *333*, 173. (b) Thomas, J. M. *Angew. Chem., Int. Ed.* **1999**, *38*, 3588. (c) Corma, A. *Chem. Rev.* **1995**, *95*, 559. (d) Li, H. L.; Eddaoudi, M.; O'Keeffe, M.; Yaghi, O. M. *Nature* **1999**, *402*, 276. (e) Kitagawa, S.; Kitaura, R.; Noro, S. *Angew. Chem., Int. Ed.* **2004**, *43*, 2334.

(2) (a) Cheetham, A. K.; Férey, G.; Loiseau, T. *Angew. Chem., Int. Ed.* **1999**, *38*, 3268. (b) Hagrman, P. J.; Hagrman, D.; Zubieta, J. *Angew. Chem., Int. Ed.* **1999**, *38*, 2638.

(3) (a) Holman, K. T.; Halihan, M.; Jurisson, M. S. S.; Atwood, J. L.; Burkhalter, R. S.; Mitchell, A. R.; Steed, J. W. *J. Am. Chem. Soc.* **1996**, *118*, 9567. (b) Tabares, L. C.; Navarro, J. A. R.; Salas, J. M. *J. Am. Chem. Soc.* **2001**, *123*, 383. (c) Vilar, R.; Mingos, D. M. P.; White, A. J. P.; Williams, D. J. *Angew. Chem., Int. Ed.* **1998**, *37*, 1258, and references cited therein.

(4) (a) Pope, M. T. *Heteropoly and Isopoly Oxometalates;* Springer-Verlag: Berlin, 1983. (b) Pope, M. T., Müller, A. *Polyoxometalate Chemistry: From Topology Via Self-Assembly to Applications;* Kluwer: New York, 2001. (c) Pope, M. T.; Müller, A. *Angew. Chem., Int. Ed. Engl.* **1991**, *30*, 34.

(5) (a) Debord, J. R. D.; Haushalter, R. C.; Meyer, L. M.; Rose, D. J.; Zapf, P. J.; Zubieta, J. *Inorg. Chim. Acta* **1997**, *256*, 165. (b) Hagrman, D.; Warren, C. J.; Haushalter, R. C.; Seip, C.; O'Connor, C. J.; Rarig, R. S.; Johnson, K. M., Jr.; Laduca, R. L., Jr.; Zubieta, J. *Chem. Mater.* **1998**, *10*, 3294. (c) Liu, C. M.; Zhang, D. Q.; Xiong, M.; Zhu, D. B. *Chem. Commun.* **2002**, 1416. (d) Lü, J.; Shen, E. H.; Li, Y. G.; Xiao, D. R.; Wang, E. B.; Xu, L. *Cryst. Growth Des.* **2005**, *5*, 65. (e) Liao, J. H.; Juang, J. S.; Lai, Y. C. *Cryst. Growth Des.* **2006**, *6*, 354. (f) Hagrman, D.; Sangregorio, C.; O'Connor, C. J.; Zubieta, J. *J. Chem. Soc., Dalton Trans.* **1998**, 3707.

(6) (a) Liu, S. X.; Xie, L. H.; Gao, B.; Zhang, C. D.; Sun, C. Y.; Li, D. H.; Su, Z. M. *Chem. Commun.* **2005**, 5023. (b) Zhang, C. D.; Liu, S. X.; Gao, B.; Sun, C. Y.; Miao, Y.; Peng, J. *Polyhedron* **2007**, *26*, 1514. (c) Zhang, L. R.; Shi, Z.; Yang, G. Y.; Chen, X. M.; Feng, S. H. *J. Chem. Soc., Dalton Trans.* **2000**, 275. (d) Lin, B. Z.; Liu, S. X. *J. Chem. Soc., Dalton Trans.* **2002**, 865.

10.1021/ic800131r CCC: $40.75 
Published on Web 07/12/2008

polyoxoanions, such as Lindquist[8] and Keggin types[9,10] or octamolybdate[11] and decavanadate clusters.[11c] Therefore, reports about POM-templated 3D MOFs are rare.[8,10,11c]

Here, we have developed the strategy of POM-templated 3D MOFs by the incorporation of a Dawson anion ($P_2W_{18}O_{62}^{6-}$) as a noncoordinating POM template around which a 3D $[M_2(bpy)_3(H_2O)_2(ox)]_n$ (M = Co(II)/Ni(II); bpy = 4,4′-bipyridine; ox = $C_2O_4^{2-}$) metal−organic framework was constructed. This strategy not only introduces one of the largest-to-date noncoordinating polyoxoanions in coordination polymer structures but also designs novel metal−ox−bpy host frameworks. The Dawson anions are uniformly buried in the host framework. Even if polyoxoanions are accommodated in the frameworks then there are some obvious spaces that create opportunities to use the redox properties of the polyoxoanions to carry out chemical reactions within the voids, avoiding a disruption of the framework topology and crystallinity.[10a]

The Dawson-type anion ($[M_{18}O_{54}(XO_4)_2]^{m-}$; M = Mo or W and X = P, As, S, or V), which was used as a template in this Article, was discovered over 50 years ago and since then has been the subject of hundreds of papers.[12,13] Given the nanometric size and the high charge of the Dawson anion, it is quite appealing and challenging to design and construct Dawson-templated MOFs. Of course, one of the major problems to overcome is the nanoscopic dimensions of the Dawson anion ($8 \times 10 \times 12$ Å$^3$), which is obviously large compared to a commonly used linear rigid ligand such as 4,4′-bipyridine (7 Å).

To overcome the obstacle and construct a host framework with a higher capacity, two possible strategies could be developed:[14] (a) The use of long links that increase the spacing between metal vertices in a net yields void space that is proportional to the length of the linker in a process called expansion. Although in principle such expanded structures provide large pores, in practice it is difficult to choose a proper rigid ligand to construct the framework for the nanosized Dawson anions. (b) The replacement of a vertex of a framework net by a group of vertices in a process termed decoration. Herein, we adopted the second synthesis approach by utilizing an oxalate-bridged binuclear superoctahedra unit, $(MN_3O)_2(C_2O_4)$, as the group of vertices, which was inspired by the work of Yaghi et al. who demonstrated the utility of metal carboxylate secondary building units (SBUs). The term SBUs has been used for some time to describe conceptual fragments of zeolites, and in reticular chemistry it refers to the geometry of the units defined by the points of extension. In our compounds, the oxalate ligand was used to chelate two metal ions and therefore lock together two $MO_3N_3$ octahedra into a rigid and thus directional binuclear superoctahedra unit; the points of extension define geometrical shapes referred to as SBUs, at least in a large term. The framework based on $(MN_3O)_2(C_2O_4)$ SBUs that are joined by 4,4′-bipyridine linkers has sufficient capacity and successfully accommodates the Dawson anions.

In this Article, we report the first noncoordinationing Dawson-templated 3D metal−organic host frameworks, namely, $[M_2(bpy)_3(H_2O)_2(ox)][P_2W_{18}O_{62}]\cdot 2(H_2bpy)\cdot nH_2O$ (M = Co(II), $n$ = 3 (**1**); M = Ni(II), $n$ = 2 (**2**); bpy = 4,4′-bipyridine; ox = $C_2O_4^{2-}$). The $(MN_3O)_2(C_2O_4)$ SBUs decorate vertices that are then spaced from other such units by two connected aromatic ring units. The resulting 3D frameworks have a high capacity for one of the largest noncoordinating polyoxoanions templates in the field of coordination polymers. The syntheses, structures, and magnetic and electrochemical properties of the two compounds are presented here.

## Experimental Section

**Materials and Methods.** $K_6P_2W_{18}O_{62}\cdot 14H_2O$ was prepared according to the literature[15] method and confirmed by IR spectroscopy. All of the other chemicals were obtained from commercial sources and used without further purification. Elemental analyses were performed on a PLASMA-SPEC(I) ICP atomic-emission spectrometer (P, W, Co, and Ni) and a Perkin-Elmer 2400 CHN elemental analyzer (C, H, and N). IR spectra were recorded in the range of 400−4000 cm$^{-1}$ on an Alpha Centaurt FT/IR spectrophotometer using KBr pellets. Thermogravimetric (TG) analyses were performed on a Perkin-Elmer TGA7 instrument in a $N_2$ atmosphere at a heating rate of 10 °C·min$^{-1}$. Powder X-ray diffraction measurements were performed on a Rigaku D/MAX-3 instrument with Cu Kα radiation in the angular range of $2\theta = 3-50°$ at 293 K. Magnetic susceptibility data were collected over the temperature range of 2−300 K in a magnetic field of 1000 Oe on a Quantum Design MPMS-5 SQUID magnetometer. A CHI 660 electrochemical workstation connected to a Digital-586 personal computer was used for the control of the electrochemical measurements and for data collection. A conventional three-electrode cell contained a **1**-CPE or a bare carbon paste electrode as the working electrode, Ag/AgCl as the reference electrode, and a Pt gauze as the counter electrode.

**Synthesis of $[Co_2(4,4'\text{-bpy})_3(H_2O)_2(ox)][P_2W_{18}O_{62}]2(H_2bpy)\cdot 3H_2O$ (1).** A mixture of $K_6P_2W_{18}O_{62}\cdot 14H_2O$ (0.5 g, 0.1 mmol), $Co(NO_3)_2\cdot 6H_2O$ (0.058 g, 0.2 mmol), oxalic acid dihydrate (0.01


(7) (a) Ren, Y. P.; Kong, X. J.; Hu, X. Y.; Sun, M.; Long, L. S.; Huang, R. B.; Zheng, L. S. *Inorg. Chem.* **2006**, *45*, 4016. (b) Zheng, P. Q.; Ren, Y. P.; Long, L. S.; Huang, R. B.; Zheng, L. S. *Inorg. Chem.* **2005**, *44*, 1190. (c) Dolbecq, A.; Draznieks, C. M.; Mialane, P.; Marrot, J.; Férey, G.; Sécheresse, F. *Eur. J. Inorg. Chem.* **2005**, 3009. (d) Dolbecq, A.; Mialane, P.; Lisnard, L.; Marrot, J.; Sécheresse, F. *Chem.−Eur. J.* **2003**, *9*, 2914.

(8) (a) Hagrman, D.; Hagrman, P. J.; Zubieta, J. *Angew. Chem., Int. Ed.* **1999**, *38*, 3165. (b) Wang, X. L.; Guo, Q. Y.; Li, Y. G.; Wang, E. B.; Hu, C. W.; Hu, N. H. *Inorg. Chem.* **2003**, *42*, 4135.

(9) (a) Kong, X. J.; Ren, Y. P.; Zheng, P. Q.; Long, Y. X.; Long, L. S.; Huang, R. B.; Zheng, L. S. *Inorg. Chem.* **2006**, *45*, 10702. (b) Li, Y. G.; Dai, L. M.; Wang, Y. H.; Wang, X. L.; Wang, E. B.; Su, Z. M.; Xu, L. *Chem. Commun.* **2007**, *25*, 2593.

(10) (a) Inman, C.; Knaust, J. M.; Keller, S. W. *Chem. Commun.* **2002**, 156. (b) Yang, L.; Naruke, H.; Yamase, T. *Inorg. Chem. Commum.* **2003**, *6*, 1020. (c) Wei, M. L.; He, C.; Hua, W. J.; Duan, C. Y.; Li, S. H.; Meng, Q. J. *J. Am. Chem. Soc.* **2006**, *128*, 13318. (d) Wei, M. L.; He, C.; Sun, Q. Z.; Meng, Q. J.; Duan, C. Y. *Inorg. Chem.* **2007**, *46*, 5957.

(11) (a) Hagrman, D.; Zubieta, C.; Rose, D. J.; Zubieta, J.; Haushalter, R. C. *Angew. Chem., Int. Ed. Engl.* **1997**, *36*, 873. (b) Rarig, R. S., Jr.; Zubieta, J. *J. Chem. Soc., Dalton Trans.* **2001**, 3446. (c) Zheng, L. M.; Wang, Y. S.; Wang, X. Q.; Korp, J. D.; Jacobson, A. J. *Inorg. Chem.* **2001**, *40*, 1380.

(12) Dawson, B. *Acta Crystallogr.* **1953**, *9*, 113.

(13) Baffert, C.; Boas, J. F.; Bond, A. M.; Kögerler, P.; Long, D. L.; Pilbrow, J. R.; Cronin, L. *Chem.−Eur. J.* **2006**, *12*, 8472.

(14) Eddaoudi, M.; Moler, D. B.; Li, H.; Chen, B.; Reineke, T. M.; O'Keeffe, M.; Yaghi, O. M. *Acc. Chem. Res.* **2001**, *34*, 319.

(15) Contant, R. *Inorg. Synth.* **1990**, *27*, 104–111.

g, 0.1 mmol) and 4,4′-bipyridine (0.078 g, 0.5 mmol), and $H_2O$ (10 mL) adjusted with NaOH (1.0 mol·$L^{-1}$) to pH 3.0 was sealed in a 23 mL Teflon reactor, kept under autogenous pressure at 160 °C for 5 days, and then cooled to room temperature at a rate of 10 °C·$h^{-1}$. Orange crystals were obtained in 54% yield (on the basis of W). Anal. Calcd. for $[Co_2(4,4'\text{-bpy})_3(H_2O)_2(ox)][P_2W_{18}O_{62}]2(H_2bpy)\cdot 3H_2O$: C, 11.47; H, 0.99; N, 2.57; Co, 2.17; P, 1.14; W, 60.79. Found: C, 11.32; H, 0.93; N, 2.43; Co, 2.02; P, 1.05; W, 60.60. IR (KBr, $cm^{-1}$): 3445 (s), 2360 (m), 1646 (m), 1611 (m), 1539 (m), 1490 (m), 1417 (m), 1090 (s), 954 (s), 909 (s), 784 (s), 525 (m), 472 (m).

**Synthesis of $[Ni_2(4,4'\text{-bpy})_3(H_2O)_2(ox)][P_2W_{18}O_{62}]2(H_2bpy)\cdot 2H_2O$ (2).** Compound **2** was prepared following the procedure described for compound **1**, but $Ni(NO_3)_2\cdot 6H_2O$ (0.059 g, 0.2 mmol) was used instead of $Co(NO_3)_2\cdot 6H_2O$. Cyan crystals were obtained in 46% yield (on the basis of W). Anal. Calcd. for $2[Ni_2(4,4'\text{-bpy})_3(H_2O)_2(ox)][P_2W_{18}O_{62}]2(H_2bpy)\cdot 2H_2O$: C, 11.51; H, 0.97; N, 2.58; Ni, 2.16; P, 1.14; W, 60.99. Found: C, 11.37; H, 0.90; N, 2.44; Ni, 2.01; P, 1.04; W, 60.80. IR (KBr, $cm^{-1}$): 3729 (w), 1644 (w), 1610 (w), 1538 (w), 1490 (w), 1090 (w), 955 (m), 908 (m), 783 (m), 674 (m), 521 (w).

**X-ray Crystallography.** Diffraction intensities for compounds **1** and **2** were collected on a Siemens Smart CCD with Mo Kα monochromatic radiation ($\lambda$ = 0.71073 Å) at 293 K. Linear absorption coefficients, scattering factors for atoms, and anomalous dispersion corrections were taken from *International Tables for X-ray Crystallography*. Empirical absorption corrections were applied. The structures were solved by the direct method and refined by the full-matrix least-squares method on $F^2$ by using the SHELXTL crystallographic software package. Anisotropic thermal parameters were used to refine all nonhydrogen atoms except the guest bpy molecules and disordered water molecules. In the structure, guest bpy molecules are slightly disordered and can be well modeled. Hydrogen atoms on all of the bpy molecules were placed on calculated positions and were included in the refinement riding on their respective parent atoms. For compounds **1** and **2**, hydrogen atoms of the coordinated water molecules were found by difference Fourier maps and were refined by fixing the O−H bond of 0.85 Å and the isotropic temperature factors at 1.2 times those of the attached mother oxygen atoms. Hydrogen atoms of the disordered water and protonated guest bpy molecules were not treated. The crystal data and structure refinement results of compounds **1** and **2** are summarized in Table 1. Selected bond lengths and bond angles for compounds **1** and **2** are provided in Tables S1 and S2 in the Supporting Information. The experimental and simulated X-ray powder diffraction patterns (XRPD) of compounds **1** and **2** are shown in Figure S6. The diffraction peaks on the patterns match well in position, indicating the phase purity.

## Results and Discussion

**Crystal Structures.** Single-crystal X-ray diffraction analysis reveals that compounds **1** and **2** are isomorphic with only slight differences in bond lengths, bond angles, and the number of lattice waters; compound **1** is described as an example below. Compound **1** exhibits a 3D host framework constructed from oxalate-bridged binuclear superoctahedron SBUs and bpy linkers, the voids of which are occupied by Dawson anions, guest bpy, and water molecules (Figure 1). The template $P_2W_{18}O_{62}^{6-}$ polyoxoanions possess the well-known Dawson-type structures, and all of the bond lengths and angles are within the normal ranges and are consistent with those described in the literature. In the metal−organic

**Table 1.** Crystal Data and Structural Refinements for Compounds **1** and **2**

| compounds | **1** | **2** |
|---|---|---|
| empirical formula | $Co_2C_{52}H_{54}N_{10}P_2W_{18}O_{71}$ | $Ni_2C_{52}H_{52}N_{10}P_2W_{18}O_{70}$ |
| mol wt | 5444.15 | 5425.70 |
| $T$ (K) | 293(2) | 293(2) |
| wavelength (Å) | 0.71073 | 0.71073 |
| cryst syst | monoclinic | monoclinic |
| space group | $P2(1)/m$ | $P2(1)/m$ |
| $a$ (Å) | 15.1832(7) | 15.0721(9) |
| $b$ (Å) | 24.7499(11) | 24.7694(14) |
| $c$ (Å) | 15.3308(7) | 15.1707(9) |
| $\beta$ (deg) | 111.3380(10) | 110.5410(10) |
| $V$ (Å$^3$) | 5366.1(4) | 5303.5(5) |
| $Z$ | 2 | 2 |
| $D_c$ (mg/m$^3$) | 3.369 | 3.398 |
| abs coeff ($mm^{-1}$) | 19.633 | 19.906 |
| reflns collected | 29 949 | 29 424 |
| independent reflns | 10 908 | 10 810 |
| $\theta$ range (deg) | 1.66−26.15 | 1.43−26.15 |
| GOF on $F^2$ | 1.013 | 1.005 |
| R1 [$I > 2\sigma(I)$][a] | 0.0420 | 0.0453 |
| wR2 (all data)[b] | 0.1126 | 0.1140 |

[a] $R1 = \sum(||F_o| - |F_c||)/\sum|F_o|$. [b] $wR2 = [\sum w(F_o^2 - F_c^2)^2/\sum w(F_o^2)^2]^{1/2}$.

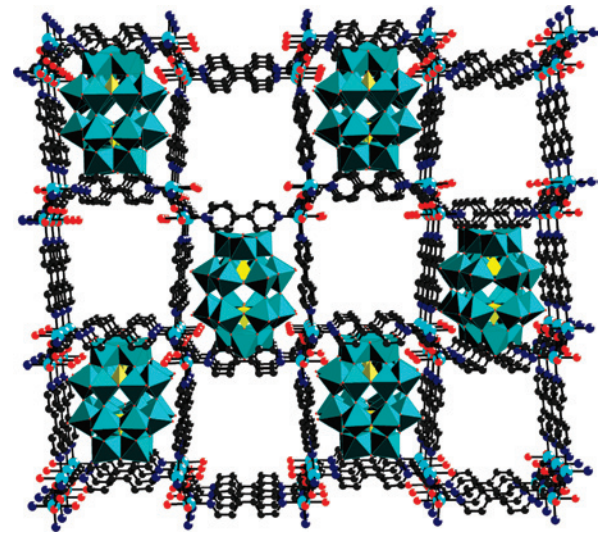

**Figure 1.** View of the 3D host framework of compound **1** with the entrained $P_2W_{18}O_{62}^{6-}$ clusters (polyhedra) along the [001] axis. Some voids are pictured empty for clarity. Hydrogen atoms, lattice water molecules, and guest bpy molecules are also omitted for clarity. Co, turquoise; O, red; N, dark-blue; C, black.

host framework, each Co(II) center coordinates with two carboxyl oxygen atoms from an oxalate (ox) ligand, three nitrogen atoms from bpy linkers, and one oxygen atom from a coordinated water molecule in a distorted octahedral geometry (Figure S1). The Co−O and Co−N distances are Co−O = 2.100(7)−2.103(8) Å; Co−$O_W$ = 2.152(8) Å; and Co−N = 2.096(9)−2.139(9) Å. Each oxalate ligand in the usual bis(bidentate) fashion chelates the two Co centers with its four carboxyl O atoms and further locks together two $CoO_3N_3$ octahedra to form a binuclear superoctahedra unit $(CoN_3O)_2(C_2O_4)$ (Figure 2); each bpy connects two identical $(CoN_3O)_2(C_2O_4)$ units. The connection of alternating binuclear superoctahedra units and bpy linkers results in an infinite 3D six-connected net. For perspicuous representation, the $(CoN_3O)_2(C_2O_4)$ units are represented by spherical SBUs, and bpy linkers are represented by sticks (Figure 3). Interestingly, the framework can be described as a distorted primitive cubic (α-Po) net in which each SBU connects six

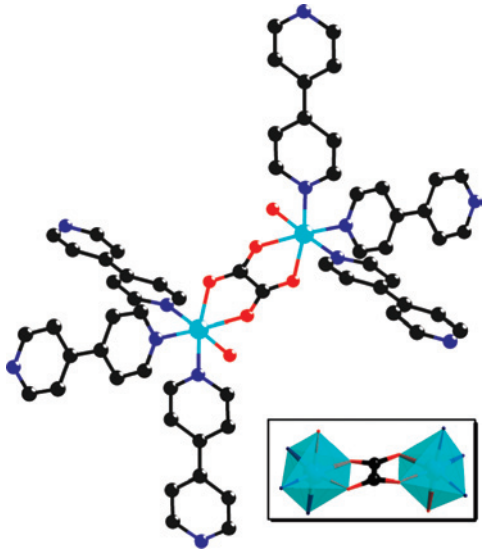

**Figure 2.** Coordination geometries of oxalate-bridged binuclear superoctahedra units in compound **1**. Hydrogen atoms are omitted for clarity. The color codes are the same as those in Figure 1.

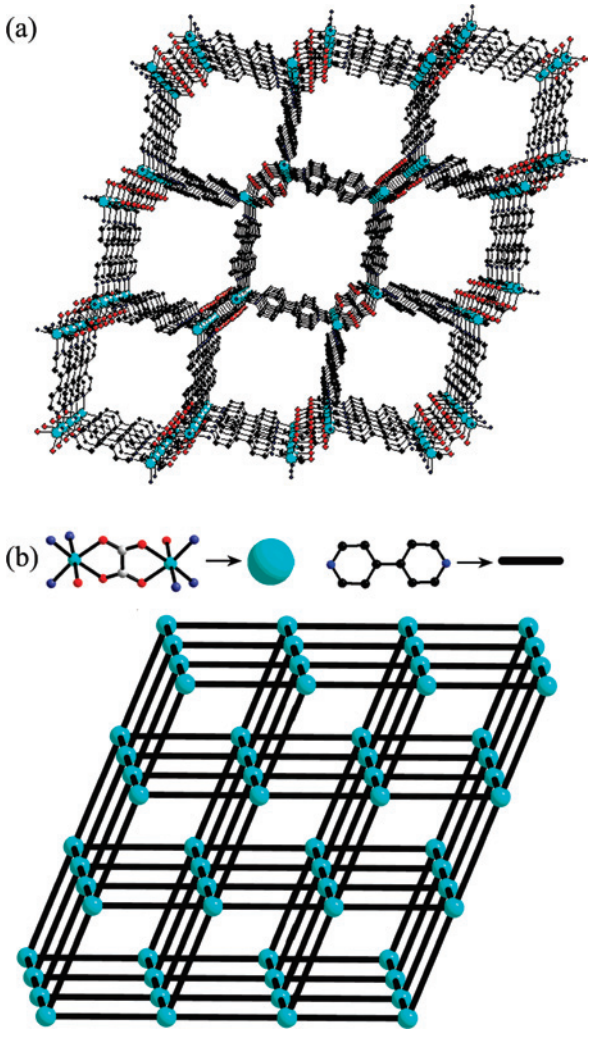


**Figure 3.** (a) Ball−stick representation of the 3D host framework of compound **1** viewed along the [010] axis and (b) representation of the distorted primitive cubic (α-Po) topology of the 3D host framework. The turquoise sphere represents the binuclear superoctahedra unit; the black stick represents the bpy linker. The color codes are the same as those in Figure 1.

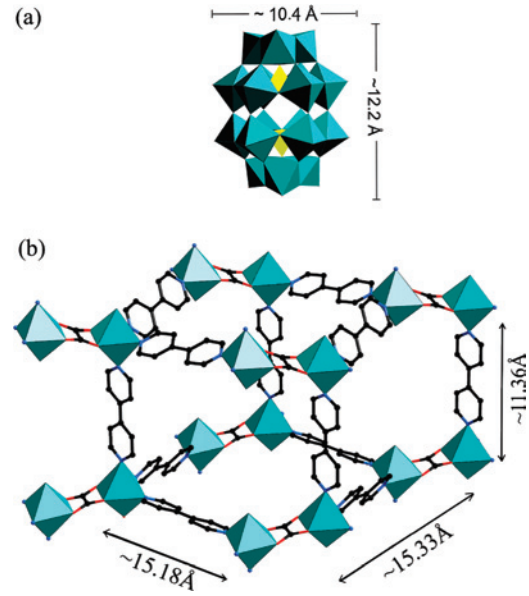


**Figure 4.** (a) Polyhedron representations of the Dawson anion and (b) view of the void size of 3D host frameworks in compound **1**. The color codes are the same as those in Figure 1.

surrounding SBU units through six bpy linkers. To the best of our knowledge, such a network in the metal−ox−bpy system has not been investigated. It is supposed that these Dawson anions serve as a template during the assembly so that hybrid cationic building blocks $[Co_2(bpy)_3(H_2O)_2(ox)]^{2+}$ are aggregated around them, leading to a framework with a large volume (Figure S2). Further studies about this intricate architecture revealed that it consists of distorted cubical cages that are constructed from 8 binuclear superoctahedra units and 12 bpy linkers with the approximate dimension of 15.33 × 15.18 × 11.36 Å$^3$ (based on the covalent volumes) (Figure 4). The cages are large enough to accommodate the Dawson anions (size: ca. 8 × 10 × 12 Å$^3$), and the template $P_2W_{18}O_{62}^{6-}$ anions uniformly fill in the cages (Figure S3). In the void of the cationic framework, the existence of approximately two protonated guest bpy molecules and three water molecules per formula that was found from the difference Fourier map is further confirmed by elemental and TG analyses. Furthermore, there exist extensive hydrogen bonds on the surfaces of oxygen atoms of Dawson anions, bpy groups, coordinated water molecules, and some lattice water molecules, which stabilize the whole crystal structure. H-bonding geometrical parameters are listed in Table S3.

**IR Spectroscopy.** In the IR spectrum of compound **1**, the characteristic peaks at 1090, 954, 909, and 784 cm$^{-1}$ are attributed to the $P_2W_{18}O_{62}^{6-}$ polyoxoanions,[16] and the characteristic bands at 1417, 1490, 1539, and 1611 cm$^{-1}$ can be regarded as features of the ring-stretching vibrations of the bpy molecules. The bands at about 1313 and 1344 cm$^{-1}$ are assigned to $\nu_s$(CO), and the broad absorption at about

(16) (a) Niu, J. Y.; Guo, D. J.; Wang, J. P.; Zhao, J. W. *Cryst. Growth Des.* **2004**, *4*, 241. (b) Niu, J. Y.; Guo, D. J.; Zhao, J. W.; Wang, J. P. *New J. Chem.* **2004**, *28*, 980.

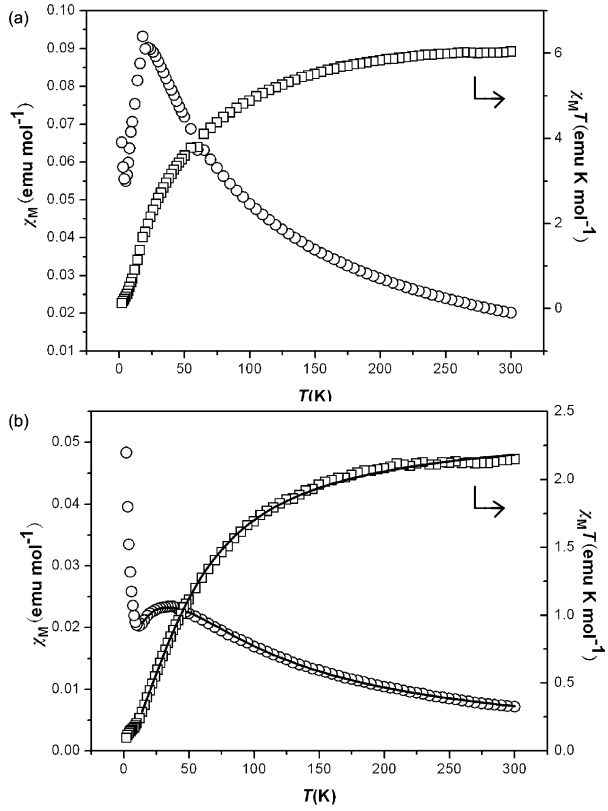


**Figure 5.** Plots of (□) the product $\chi_M T$ versus $T$ and (○) $\chi_M$ versus $T$ under an applied magnetic field of 1000 Oe for compounds (a) **1** and (b) **2**. The solid lines are theoretical fits based on the Curie−Weiss law and equation, respectively.

1640 cm$^{-1}$ corresponds to $\nu_{as}$(CO) of the oxalate ligand in a bis-bidentate bridging mode.[17] The infrared spectrum of compound **2** is similar to that of compound **1** (Figure S4).

**Thermogravimetric Analyses.** TG analyses were performed to determine the thermal stabilities of compound **1** (Figure S5). An initial weight loss of 4.05% below 200 °C is significantly higher than the value of 1.65% that was calculated for the release of the lattice water and coordination water molecules, which indicates that a number of the bpy guests were also released. The second weight loss of 3.55% covered a temperature range of 350−450 °C, indicating the release of the rest of the bpy guests. The total weight loss of 7.60% below 450 °C is close to the calculated value of 7.46% for the release of five water molecules and two bpy guests. Above 500 °C, the framework begins to collapse, which corresponds to the loss of the organic ligands (bpy and oxalate) and to the sublimation of $P_2O_5$. The total weight loss is about 20.59%, which is consistent with the calculated value of 20.48%.

**Magnetic Properties.** Magnetic susceptibilities of compounds **1** and **2** were measured in the 2−300 K temperature range. Figure 5a shows the magnetic behavior of compound **1** in the form of $\chi_M T$ versus $T$ and $\chi_M$ versus $T$ plots. At room temperature, the experimental $\chi_M T$ value is 6.04 emu·K·mol$^{-1}$ per unit higher than the expected spin-only value ($\chi_M T$ = 3.75 emu·K·mol$^{-1}$, $S$ = 3/2, assuming $g$ = 2) for two high-spin Co(II) atoms in each $Co_2$ unit per formula, which is caused by an unquenched orbital contribution arising from the $^4T_{1g}$ ground state of Co(II).[18] As the system cools, $\chi_M T$ smoothly decreases over the entire temperature region. In the plot of $\chi_M$ versus $T$, a maximum at 18 K was observed, which is the nature of the typical antiferromagnetic interaction between the magnetic centers. In the low-temperature region below 5 K, the increase in the magnetic susceptibility suggests the presence of the paramagnetic impurities in this compound.[19]

The plot of the temperature dependence of the magnetic properties of compound **2** is similar to that of compound **1** (see Figure 5b). At room temperature, the experimental $\chi_M T$ value is 2.14 emu·K·mol$^{-1}$ per unit, which is slightly higher than the expected spin-only value ($\chi_M T$ = 2.00 emu·K·mol$^{-1}$, $S$ = 1, assuming $g$ = 2) for two high-spin Ni(II) atoms in each $Ni_2$ unit per formula. Upon cooling, $\chi_M T$ steadily decreases from 300 to 2 K. A linear fitting of the reciprocal of susceptibility ($1/\chi_M$) versus the temperature curve with the Curie−Weiss law in the range of 100−300 K gives values of $C$ = 2.45 emu·K·mol$^{-1}$ and $\theta$ = −39.32 K (Figure S8). Furthermore, in the plot of $\chi_M$ versus $T$, a large, broad protuberance with a maximum at 36 K was observed, which also indicates the antiferromagnetic coupling between Ni(II) ions. In the low-temperature region below 12 K, paramagnetic impurities result in an increase in the magnetic susceptibility that is similar to that of compound **1**. To estimate the coupling interaction between the Ni(II) atoms, we neglected the coupling interactions between the metal centers separated by the 4,4′-bpy linkers and only considered the contribution of the magnetic exchange in each binuclear metal oxalate unit ([$Ni_2$(ox)]). The intramolecular exchange interactions can be represented by the isotropic spin Hamiltonian equation

$$\hat{H} = -J\hat{S}_A \cdot \hat{S}_B \quad (1)$$

where $J$ is the exchange integral and $S_A = S_B = 1$. The magnetic susceptibility was analyzed by using eq 2 as follows

$$\chi_M = \left(\frac{2Ng^2\beta^2}{kT}\right)\left(\frac{[\exp(J/kT) + 5\exp(J/kT)](1-\rho)}{1 + 3\exp(J/kT) + 5\exp(J/kT)}\right) + \frac{4Ng^2\beta^2\rho}{3kT} \quad (2)$$

This equation has been modified to take into account the admixture of paramagnetic impurities, where $N$, $\beta$, $k$, and $T$ have their usual meanings, $\rho$ is the fraction of the noncoupled impurity, and $g$ is the $g$ factor of the dinuclear nickel complexes. The experimental data can be fitted over the temperature range of 14−300 K (see Figure 5b), and the following set of parameters was obtained: $J$ = −32.39 cm$^{-1}$, $g$ = 2.20, $\rho$ = 0.074, and $R = 4.0 \times 10^{-4}$ ($R = \sum[(\chi_M T)_{calcd} - (\chi_M T)_{obsd}]^2/\sum(\chi_M T)_{obsd}^2$), which is consistent with the antiferromagnetic interactions deduced from the plot. To the best of our knowledge, antiferromagntic coupling interactions

(17) Tuero, L. S.; Garcia-Lozano, J.; Monto, E. E.; Borja, M. B.; Dahan, F.; Tuchagues, J.-P.; Legros, J.-P. *J. Chem. Soc., Dalton Trans.* **1991**, 2619.

(18) Sun, C. Y.; Zheng, X. J.; Gao, S.; Li, L. C.; Jin, L. P. *Eur. J. Inorg. Chem.* **2005**, 4150.

(19) Zhao, W.; Song, Y.; Taka-aki, O.; Fan, J.; Sun, W. Y.; Norikazu, U. *Inorg. Chem.* **2005**, *44*, 3330.

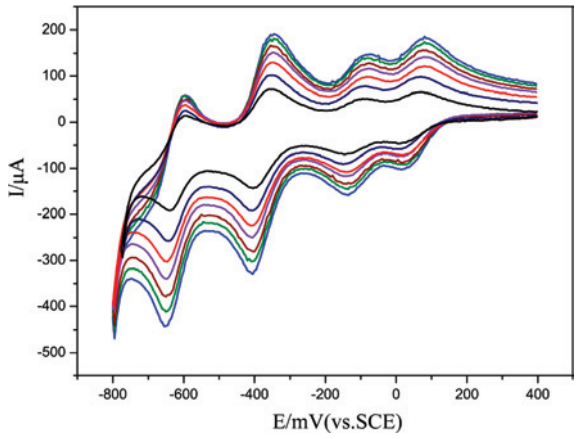


**Figure 6.** Cyclic voltammograms of **1**-CPE in a 1 M HCl solution at different scan rates (from inner to outer: 50, 90, 150, 200, 250, 300, and 350 $mV \cdot s^{-1}$).

have been observed in other structurally relevant dinuclear Ni(II) oxalate-bridged complexes,[20] and the observed *J* values of compound **2** are close to those previously reported.

**Electrochemical Properties.** The electrochemical behavior of **1**-CPE and its electrocatalytic reduction of nitrite were also investigated by cyclic voltammetry (CV). Four well-defined redox couples with approximate electron ratios of 1:1:2:2 can be observed in a 1 M aqueous HCl solution attributable to the $P_2W_{18}O_{40}^{3-}$ polyoxoanions (Figure 6), which are identical to the dissolved species in the electrolyte solution.[21] The approximate proportionality of the reduction peak current to the scan rate up to 350 $mV \cdot s^{-1}$ indicates that the redox process is surface-controlled.[22]

**1**-CPE is very stable. When the potential range is maintained between 400 and −800 mV, the peak currents remain almost unchanged after hundreds of cycles. After **1**-CPE was stored at room temperature for 1 month, the peak current decreased only slightly and could be renewed by squeezing a little carbon paste out of the tube. Thus, **1**-CPE could be an ideal electrode material for investigating electrocatalytic properties. Actually, **1**-CPE was tested for its activity in the reduction of nitrite (see the Supporting Information). The electroreduction of nitrite requires a large overpotential;[23] therefore, no obvious response is observed in the range of 400 to −800 mV on a bare CPE in 1 M HCl containing 1 mM $NaNO_2$. However, **1**-CPE has electrocatalytic activity toward the reduction of nitrite. Upon the addition of $NO_2^-$, the first reduction peak current increases while the corresponding oxidation peak current decreases, which suggests that nitrite is reduced by one-electron-reduced species. It is consistent with that for $K_6P_2W_{18}O_{62}$ deposited on the multilayer films, where one-electron-reduced $P_2W_{18}O_{62}^{6-}$ possesses electrocatalytic activity for the $H_2O_2$ reduction.[24]

## Conclusions

In short, through the successful introduction of binuclear superoctahedron SBUs, we developed the strategy of POMs-templated 3D MOFs by the incorporation of the nanosized Dawson anion as a noncoordinating polyoxoanions template. The resulting materials exhibit not only the nature of the typical antiferromagnetism of host frameworks but also the electrochemical activation of POMs. In the future, we will explore the applications of the title compounds, such as in catalysis and separation, and will further develop the strategy of combining SBUs with POM templates on the trail of the rational design of multifunctional materials.

**Acknowledgment.** This work was supported by the National Science Foundation of China (grant no. 20571014), the Program for New Century Excellent Talents in University (NCET-07-0169), and the Analysis and Testing Foundation of Northeast Normal University.

**Supporting Information Available:** X-ray crystallographic data for compounds **1** and **2**; XRPD patterns; IR spectra; TG curve; magnetic curves; and CV spectrum. This material is available free of charge via the Internet at http://pubs.acs.org.

IC800131R

(20) (a) Ball, P. W.; Blake, A. B. *J. Chem. Soc. A* **1969**, 1415. (b) Duggan, M. D.; Barefield, E. K.; Hendrickson, D. N. *Inorg. Chem.* **1973**, *12*, 985. (c) Battaglia, L. P.; Bianchi, A.; Corradi, A. B.; Garcia-España, E.; Micheloni, M.; Julve, M. *Inorg. Chem.* **1988**, *27*, 4174. (d) Bencini, A.; Bianchi, A.; Garcia-España, E.; Jeannin, Y.; Julve, M.; Marcelino, V.; Philoche-Levisalles, M. *Inorg. Chem.* **1990**, *29*, 963. (e) McLachlan, G. A.; Fallon, G. D.; Martin, R. L.; Moubaraki, B.; Murray, K. S.; Spiccia, L. *Inorg. Chem.* **1994**, *33*, 4663.
(21) Sadakane, M.; Steckhan, E. *Chem. Rev.* **1998**, *98*, 219.
(22) Cheng, L.; Zhang, X. M.; Xi, X. D.; Dong, S. J. *J. Electroanal. Chem.* **1996**, *407*, 97.
(23) Keita, B.; Nadjo, L. *J. Electroanal. Chem.* **1987**, *227*, 77.
(24) Shen, Y.; Liu, J. Y.; Jiang, J. G.; Liu, B. F.; Dong, S. J. *Electroanalysis* **2002**, *14*, 1557.